

Muon conversion to electron in nuclei in Minimal R-symmetric Supersymmetric Standard Model

Ke-Sheng Sun^{a*}, Sheng-Kai Cui^{b†}, Wei Li^{b‡}, Hai-Bin Zhang^{b§}

^a*Department of Physics, Baoding University, Baoding 071000, China*

^b*Department of Physics, Hebei University, Baoding 071002, China*

Abstract

We analyze the lepton flavor violating process $\mu - e$ conversion in the framework of the minimal R-symmetric supersymmetric standard model. The theoretical predictions are determined by considering the experimental constraint on parameter δ^{12} from the lepton flavor violating decay $\mu \rightarrow e\gamma$. The numerical results show that γ penguins and Z penguins dominate the predictions on $\text{CR}(\mu - e, \text{Nucleus})$, and the contributions from Higgs penguins and box diagrams are insignificant. The theoretical predictions on conversion rate $\text{CR}(\mu - e, \text{Nucleus})$ in a Al or Ti target can be enhanced close to the future experimental sensitivities and are very promising to be observed in near future experiment.

PACS numbers: 13.35.Bv, 12.60.Jv

Keywords: Lepton flavor violating, R-symmetry, MRSSM

* sunkesheng@126.com

† 2252953633@qq.com

‡ watliwei@163.com

§ hbzhang@hbu.edu.cn

I. INTRODUCTION

Searching for Lepton Flavor Violating (LFV) decays are of great importance in probing New Physics (NP) beyond the Standard Model (SM) in which the theoretical predictions on those LFV decays are suppressed by small masses of neutrinos and far beyond the experimental accessibility. There are many different ways to search LFV such as $\mu \rightarrow e\gamma$, $\mu \rightarrow 3e$, $\mu - e$ conversion in nucleus, τ decays, hadron decays and so on. However, no LFV signals have been observed in experiment up to now. The $\mu - e$ conversion in nucleus is a process that muons are captured in a target of atomic nucleus and form a muonic atom. Several experiments have been built or planned to built to search for this process. Current limit on the $\mu - e$ conversion rate is 4.6×10^{-12} for a Ti target at TRIUMF [1], 4.3×10^{-12} for a Ti target and 7×10^{-13} for a Au target at SINDRUM-II experiment [2]. In future, this LFV process may be observed by experiments with improved sensitivity. A future prospects of 10^{-13} for a C target or 10^{-14} for a SiC target at DeeMe [3], 10^{-18} for a Ti target at PRISM [4] and $10^{-16} - 10^{-17}$ for a Al target at Mu2e and COMET [5, 6] will be achieved, which improve the current experimental limits by several orders of magnitude.

The $\mu - e$ conversion rate has been calculated in the literature for various extensions of SM. Some seesaw models with right handed neutrinos [7–13], scalar triplets [14–16], fermion singlet [17] and fermion triplets [18], can have $\text{CR}(\mu - e, \text{Nucleus})$ close to the experimental sensitivity. There are a few studies within models of non-SUSY, such as unparticle model [19, 20], littlest Higgs model [21, 22], left-right symmetric models [23], 331 model [24] and so on. There are also a few studies within models of SUSY, such as MSSM [25], R-parity violating SUSY [26], low-scale seesaw models of minimal supergravity [27], BLMSSM [28, 29], the CMSSM-seesaw [30], $\mu\nu$ SSM [31] and so on. Some pedagogical introductions on the theoretical motivations for charged LFV and the experimental aspects is provided in Ref. [32–34].

In this paper, we will study the LFV process $\mu - e$ conversion in the Minimal R-symmetric Supersymmetric Standard Model (MRSSM) [35]. The MRSSM has an unbroken global $U(1)_R$ symmetry and provides a new solution to the supersymmetric flavor problem in MSSM. In this model, R-symmetry forbids Majorana gaugino masses, μ term, A terms and all left-right squark and slepton mass mixings. The R -charged Higgs $SU(2)_L$ doublets \hat{R}_u

and \hat{R}_d are introduced in MRSSM to yield the Dirac mass terms of higgsinos. Additional superfields \hat{S} , \hat{T} and \hat{O} are introduced to yield Dirac mass terms of gauginos. Studies on phenomenology in MRSSM can be found in literatures [36–54]. Similar to MSSM, the off-diagonal entries δ^{ij} in slepton mass matrices m_l^2 and m_r^2 dominate the LFV process $\mu - e$ conversion. Taking account of the constraints from radiative decays $\mu \rightarrow e\gamma$ on the off-diagonal parameters δ^{ij} , we explore $\mu - e$ conversion rate as a function of off-diagonal parameter δ^{ij} and other model parameters.

The paper is organized as follows. In Section II, we present the details of the MRSSM. All relevant mass matrices and mixing matrices are provided. Feynman diagrams contributing to $\mu - e$ conversion in MRSSM are given at one loop level. The $\mu - e$ conversion rate are computed in effective Lagrangian method, and notations and conventions for effective operators and Wilson coefficients are also listed. The numerical results are presented in Section III, and the conclusion is drawn in Section IV.

II. MRSSM

In this section, we firstly provide a simple overview of MRSSM in order to fix the notations we use in this paper. The MRSSM has the same gauge symmetry $SU(3)_C \times SU(2)_L \times U(1)_Y$ as the SM and MSSM. The spectrum of fields in MRSSM contains the standard MSSM matter, Higgs and gauge superfields augmented by chiral adjoints \hat{O} , \hat{T} , \hat{S} and two R -Higgs iso-doublets. The general form of the superpotential of the MRSSM is given by [36]

$$\begin{aligned} \mathcal{W}_{MRSSM} = & \mu_d(\hat{R}_d\hat{H}_d) + \mu_u(\hat{R}_u\hat{H}_u) + \Lambda_d(\hat{R}_d\hat{T})\hat{H}_d + \Lambda_u(\hat{R}_u\hat{T})\hat{H}_u + \lambda_d\hat{S}(\hat{R}_d\hat{H}_d) \\ & + \lambda_u\hat{S}(\hat{R}_u\hat{H}_u) - Y_d\hat{d}(\hat{q}\hat{H}_d) - Y_e\hat{e}(\hat{l}\hat{H}_d) + Y_u\hat{u}(\hat{q}\hat{H}_u), \end{aligned} \quad (1)$$

where \hat{H}_u and \hat{H}_d are the MSSM-like Higgs weak iso-doublets, \hat{R}_u and \hat{R}_d are the R -charged Higgs $SU(2)_L$ doublets and the corresponding Dirac higgsino mass parameters are denoted as μ_u and μ_d . Although R -symmetry forbids the μ terms of the MSSM, the bilinear combinations of the normal Higgs $SU(2)_L$ doublets \hat{H}_u and \hat{H}_d with the Higgs $SU(2)_L$ doublets \hat{R}_u and \hat{R}_d are allowed in Eq.(1). Parameters λ_u , λ_d , Λ_u and Λ_d are Yukawa-like trilinear terms involving the singlet \hat{S} and the triplet \hat{T} . For our phenomenological studies we take

the soft-breaking terms involving scalar mass that have been considered in [38]

$$\begin{aligned}
V_{SB,S} = & m_{H_d}^2(|H_d^0|^2 + |H_d^-|^2) + m_{H_u}^2(|H_u^0|^2 + |H_u^+|^2) + (B_\mu(H_d^-H_u^+ - H_d^0H_u^0) + h.c.) \\
& + m_{R_d}^2(|R_d^0|^2 + |R_d^+|^2) + m_{R_u}^2(|R_u^0|^2 + |R_u^-|^2) + m_T^2(|T^0|^2 + |T^-|^2 + |T^+|^2) \\
& + m_S^2|S|^2 + m_O^2|O|^2 + \tilde{d}_{L,i}^* m_{q,ij}^2 \tilde{d}_{L,j} + \tilde{d}_{R,i}^* m_{d,ij}^2 \tilde{d}_{R,j} + \tilde{u}_{L,i}^* m_{q,ij}^2 \tilde{u}_{L,j} \\
& + \tilde{u}_{R,i}^* m_{u,ij}^2 \tilde{u}_{R,j} + \tilde{e}_{L,i}^* m_{l,ij}^2 \tilde{e}_{L,j} + \tilde{e}_{R,i}^* m_{r,ij}^2 \tilde{e}_{R,j} + \tilde{\nu}_{L,i}^* m_{l,ij}^2 \tilde{\nu}_{L,j}.
\end{aligned} \tag{2}$$

All trilinear scalar couplings involving Higgs bosons to squarks and sleptons are forbidden in Eq.(2) cause the sfermions have an R-charge and these terms are non R-invariant, and this relaxes the flavor problem of the MSSM [35]. The Dirac nature is a manifest feature of MRSSM fermions and the soft-breaking Dirac mass terms of the singlet \hat{S} , triplet \hat{T} and octet \hat{O} take the form as

$$V_{SB,DG} = M_D^B \tilde{B} \tilde{S} + M_D^W \tilde{W}^a \tilde{T}^a + M_D^O \tilde{g} \tilde{O} + h.c., \tag{3}$$

where \tilde{B} , \tilde{W} and \tilde{g} are usually MSSM Weyl fermions. R-Higgs bosons do not develop vacuum expectation values since they carry R-charge 2. After electroweak symmetry breaking the singlet and triplet vacuum expectation values effectively modify the μ_u and μ_d , and the modified μ_i parameters are given by

$$\mu_d^{eff,+} = \frac{1}{2} \Lambda_d v_T + \frac{1}{\sqrt{2}} \lambda_d v_S + \mu_d, \quad \mu_u^{eff,-} = -\frac{1}{2} \Lambda_u v_T + \frac{1}{\sqrt{2}} \lambda_u v_S + \mu_u.$$

The v_T and v_S are vacuum expectation values of \hat{T} and \hat{S} which carry R-charge zero.

In the weak basis $(\sigma_d, \sigma_u, \sigma_S, \sigma_T)$, the pseudo-scalar Higgs boson mass matrix and the diagonalization procedure are

$$\mathcal{M}_{A^0} = \begin{pmatrix} B_\mu \frac{v_u}{v_d} & B_\mu & 0 & 0 \\ B_\mu & B_\mu \frac{v_d}{v_u} & 0 & 0 \\ 0 & 0 & m_S^2 + \frac{\lambda_d^2 v_d^2 + \lambda_u^2 v_u^2}{2} & \frac{\lambda_d \Lambda_d v_d^2 - \lambda_u \Lambda_u v_u^2}{2\sqrt{2}} \\ 0 & 0 & \frac{\lambda_d \Lambda_d v_d^2 - \lambda_u \Lambda_u v_u^2}{2\sqrt{2}} & m_T^2 + \frac{\Lambda_d^2 v_d^2 + \Lambda_u^2 v_u^2}{4} \end{pmatrix}, \quad Z^A \mathcal{M}_{A^0} (Z^A)^\dagger = \mathcal{M}_{A^0}^{\text{diag}}. \tag{4}$$

In the weak basis $(\phi_d, \phi_u, \phi_S, \phi_T)$, the scalar Higgs boson mass matrix and the diagonalization procedure are

$$\mathcal{M}_h = \begin{pmatrix} \mathcal{M}_{11} & \mathcal{M}_{21}^T \\ \mathcal{M}_{21} & \mathcal{M}_{22} \end{pmatrix}, \quad Z^h \mathcal{M}_h (Z^h)^\dagger = \mathcal{M}_h^{\text{diag}}, \tag{5}$$

where the submatrices ($c_\beta = \cos\beta$, $s_\beta = \sin\beta$) are

$$\begin{aligned}\mathcal{M}_{11} &= \begin{pmatrix} m_Z^2 c_\beta^2 + m_A^2 s_\beta^2 & -(m_Z^2 + m_A^2) s_\beta c_\beta \\ -(m_Z^2 + m_A^2) s_\beta c_\beta & m_Z^2 s_\beta^2 + m_A^2 c_\beta^2 \end{pmatrix}, \\ \mathcal{M}_{21} &= \begin{pmatrix} v_d(\sqrt{2}\lambda_d\mu_d^{eff,+} - g_1 M_B^D) & v_u(\sqrt{2}\lambda_u\mu_u^{eff,-} + g_1 M_B^D) \\ v_d(\Lambda_d\mu_d^{eff,+} + g_2 M_W^D) & -v_u(\Lambda_u\mu_u^{eff,1} + g_2 M_W^D) \end{pmatrix}, \\ \mathcal{M}_{22} &= \begin{pmatrix} 4(M_B^D)^2 + m_S^2 + \frac{\lambda_d^2 v_d^2 + \lambda_u^2 v_u^2}{2} & \frac{\lambda_d \Lambda_d v_d^2 - \lambda_u \Lambda_u v_u^2}{2\sqrt{2}} \\ \frac{\lambda_d \Lambda_d v_d^2 - \lambda_u \Lambda_u v_u^2}{2\sqrt{2}} & 4(M_W^D)^2 + m_T^2 + \frac{\Lambda_d^2 v_d^2 + \Lambda_u^2 v_u^2}{4} \end{pmatrix}.\end{aligned}$$

The number of neutralino degrees of freedom in MRSSM is doubled compared to MSSM as the neutralinos are Dirac-type. In the weak basis of four neutral electroweak two-component fermions $\xi_i = (\tilde{B}, \tilde{W}^0, \tilde{R}_d^0, \tilde{R}_u^0)$ with R-charge 1 and four neutral electroweak two-component fermions $\varsigma_i = (\tilde{S}, \tilde{T}^0, \tilde{H}_d^0, \tilde{H}_u^0)$ with R-charge -1, the neutralino mass matrix and the diagonalization procedure are

$$m_{\chi^0} = \begin{pmatrix} M_B^D & 0 & -\frac{1}{2}g_1 v_d & \frac{1}{2}g_1 v_u \\ 0 & M_W^D & \frac{1}{2}g_2 v_d & -\frac{1}{2}g_2 v_u \\ -\frac{1}{\sqrt{2}}\lambda_d v_d & -\frac{1}{2}\Lambda_d v_d & -\mu_d^{eff,+} & 0 \\ \frac{1}{\sqrt{2}}\lambda_u v_u & -\frac{1}{2}\Lambda_u v_u & 0 & \mu_u^{eff,-} \end{pmatrix}, (N^1)^* m_{\chi^0} (N^2)^\dagger = m_{\chi^0}^{\text{diag}}. \quad (6)$$

The mass eigenstates κ_i and φ_i , and physical four-component Dirac neutralinos are

$$\xi_i = \sum_{j=1}^4 (N_{ji}^1)^* \kappa_j, \varsigma_i = \sum_{j=1}^4 (N_{ij}^2)^* \varphi_j, \chi_i^0 = \begin{pmatrix} \kappa_i \\ \varphi_i^* \end{pmatrix}.$$

The number of chargino degrees of freedom in MRSSM is also doubled compared to MSSM and these charginos can be grouped to two separated chargino sectors according to their R-charge. The χ^\pm -charginos sector has R-charge 1 electric charge; the ρ -charginos sector has R-charge -1 electric charge. In the basis $\xi_i^+ = (\tilde{W}^+, \tilde{R}_d^+)$ and $\varsigma_i^- = (\tilde{T}^-, \tilde{H}_d^-)$, the χ^\pm -charginos mass matrix and the diagonalization procedure are

$$m_{\chi^\pm} = \begin{pmatrix} g_2 v_T + M_D^W & \frac{1}{\sqrt{2}}\Lambda_d v_d \\ \frac{1}{\sqrt{2}}g_2 v_d & -\frac{1}{2}\Lambda_d v_T + \frac{1}{\sqrt{2}}\lambda_d v_S + \mu_d \end{pmatrix}, (U^1)^* m_{\chi^\pm} (V^1)^\dagger = m_{\chi^\pm}^{\text{diag}}. \quad (7)$$

The mass eigenstates λ_i^\pm and physical four-component Dirac charginos are

$$\xi_i^+ = \sum_{j=1}^2 (V_{ij}^1)^* \lambda_j^+, \varsigma_i^- = \sum_{j=1}^2 (U_{ji}^1)^* \lambda_j^-, \chi_i^\pm = \begin{pmatrix} \lambda_i^+ \\ \lambda_i^{-*} \end{pmatrix}.$$

Here, we don't discuss the ρ -charginos sector in detail since it doesn't contribute to $\mu - e$ conversion. More information about the ρ -charginos can be found in Ref.[38, 40, 42, 52].

In MRSSM the LFV decays mainly originate from the potential misalignment in sleptons mass matrices. In the gauge eigenstate basis $\tilde{\nu}_{iL}$, the sneutrino mass matrix and the diagonalization procedure are

$$m_{\tilde{\nu}}^2 = m_l^2 + \frac{1}{8}(g_1^2 + g_2^2)(v_d^2 - v_u^2) + g_2 v_T M_D^W - g_1 v_S M_D^B, Z^V m_{\tilde{\nu}}^2 (Z^V)^\dagger = m_{\tilde{\nu}}^{2,\text{diag}}, \quad (8)$$

where the last two terms in mass matrix are newly introduced by MRSSM. The slepton mass matrix and the diagonalization procedure are

$$\begin{aligned} m_{\tilde{e}}^2 &= \begin{pmatrix} (m_{\tilde{e}}^2)_{LL} & 0 \\ 0 & (m_{\tilde{e}}^2)_{RR} \end{pmatrix}, Z^E m_{\tilde{e}}^2 (Z^E)^\dagger = m_{\tilde{e}}^{2,\text{diag}}, \\ (m_{\tilde{e}}^2)_{LL} &= m_l^2 + \frac{1}{2}v_d^2 |Y_e|^2 + \frac{1}{8}(g_1^2 - g_2^2)(v_d^2 - v_u^2) - g_1 v_S M_D^B - g_2 v_T M_D^W, \\ (m_{\tilde{e}}^2)_{RR} &= m_r^2 + \frac{1}{2}v_d^2 |Y_e|^2 + \frac{1}{4}g_1^2(v_u^2 - v_d^2) + 2g_1 v_S M_D^B. \end{aligned} \quad (9)$$

The sources of LFV are the off-diagonal entries of the 3×3 soft supersymmetry breaking matrices m_l^2 and m_r^2 in Eqs.(8, 9). From Eq.(9) we can see that the left-right slepton mass mixing is absent in MRSSM, whereas the A terms are present in MSSM.

The mass matrix for up squarks and down squarks, and the relevant diagonalization procedure are

$$\begin{aligned} m_{\tilde{u}}^2 &= \begin{pmatrix} (m_{\tilde{u}}^2)_{LL} & 0 \\ 0 & (m_{\tilde{u}}^2)_{RR} \end{pmatrix}, Z^U m_{\tilde{u}}^2 (Z^U)^\dagger = m_{\tilde{u}}^{2,\text{diag}}, \\ m_{\tilde{d}}^2 &= \begin{pmatrix} (m_{\tilde{d}}^2)_{LL} & 0 \\ 0 & (m_{\tilde{d}}^2)_{RR} \end{pmatrix}, Z^D m_{\tilde{d}}^2 (Z^D)^\dagger = m_{\tilde{d}}^{2,\text{diag}}, \\ (m_{\tilde{u}}^2)_{LL} &= m_q^2 + \frac{1}{2}v_u^2 |Y_u|^2 + \frac{1}{24}(g_1^2 - 3g_2^2)(v_u^2 - v_d^2) + \frac{1}{3}g_1 v_S M_D^B + g_2 v_T M_D^W, \\ (m_{\tilde{u}}^2)_{RR} &= m_u^2 + \frac{1}{2}v_u^2 |Y_u|^2 + \frac{1}{6}g_1^2(v_d^2 - v_u^2) - \frac{4}{3}g_1 v_S M_D^B, \\ (m_{\tilde{d}}^2)_{LL} &= m_q^2 + \frac{1}{2}v_d^2 |Y_d|^2 + \frac{1}{24}(g_1^2 + 3g_2^2)(v_u^2 - v_d^2) + \frac{1}{3}g_1 v_S M_D^B - g_2 v_T M_D^W, \\ (m_{\tilde{d}}^2)_{RR} &= m_d^2 + \frac{1}{2}v_d^2 |Y_d|^2 + \frac{1}{12}g_1^2(v_u^2 - v_d^2) + \frac{2}{3}g_1 v_S M_D^B. \end{aligned} \quad (10)$$

The MRSSM has been implemented in the Mathematica package SARAH [55–57], and we use the Feynman rules generated with SARAH-4.14.3 in our work. In MRSSM, violating of lepton flavor arises at the one loop level. In MRSSM, $\mu - e$ conversion is induced by the Feynman diagrams given in FIG.1. The various contributions to this process can be

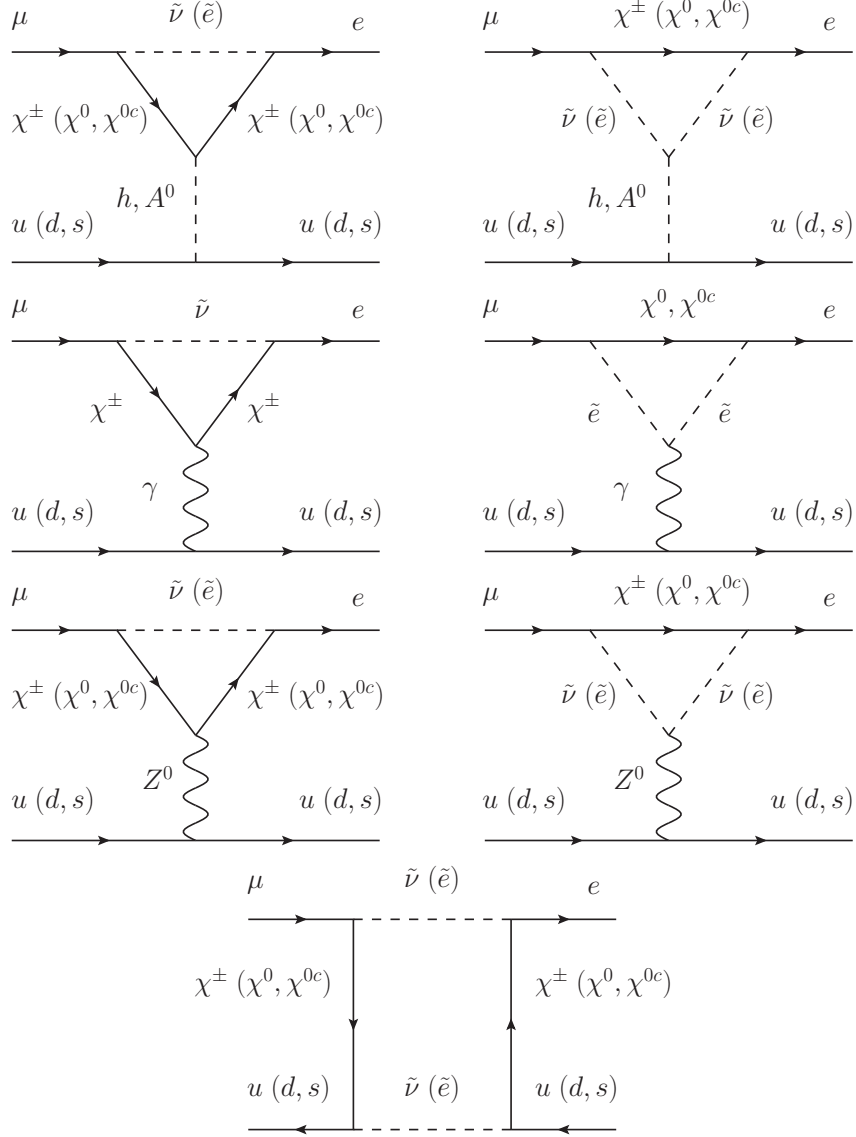


FIG. 1: One loop Feynman diagrams contributing to $\mu - e$ conversion in MRSSM.

classified into Higgs penguins, γ penguins, Z penguins and box diagrams. In the effective Lagrangian method, one can derive the effective Lagrangian relevant for $\mu - e$ conversion as [58]

$$\begin{aligned}
\mathcal{L}_{eff} = & e \bar{l}_e \gamma^\mu \left(K_1^L P_L + K_1^R P_R \right) l_\mu A_\mu + \sum_{K=S,V}^{X,Y=L,R} B_{XY}^K \bar{l}_e \Gamma_K P_X l_\mu \bar{d} \Gamma_K P_Y d \\
& + \sum_{K=S,V}^{X,Y=L,R} C_{XY}^K \bar{l}_e \Gamma_K P_X l_\mu \bar{u} \Gamma_K P_Y u + h.c.
\end{aligned} \tag{11}$$

The conversion rate $CR(\mu - e, Nucleus)$ in nuclei can be calculated by

$$CR(\mu - e, Nucleus) = \sum_{X=L,R} \frac{p_e E_e m_\mu^3 G_F^2 \alpha^3 Z_{eff}^4 F_p^2}{8\pi^2 Z \Gamma_{capt}} \times \left| (Z + N) \left(g_{XV}^{(0)} + g_{XS}^{(0)} \right) + (Z - N) \left(g_{XV}^{(1)} + g_{XS}^{(1)} \right) \right|^2. \quad (12)$$

Here p_e and E_e ($\sim m_\mu$ in the numerical evaluation) are the momentum and energy of the electron. G_F and α are the Fermi constant and the fine structure constant, respectively. Z_{eff} is the effective atomic charge. Z and N are the number of protons and neutrons in the nucleus. F_p is the nuclear form factor and Γ_{capt} is the total muon capture rate. The values of Z_{eff} , F_p and Γ_{capt} that will be used in the phenomenological analysis below are given in Table. I. At quark level, the $g_{XK}^{(i)}$ factors (with $i=0,1$, $X=L,R$ and $K=S,V$) can be written as combinations of effective couplings

$$g_{XK}^{(i)} = \frac{1}{2} \sum_{q=u,d,s} \left(g_{XK(q)} G_K^{(q,p)} + (-1)^i g_{XK(q)} G_K^{(q,n)} \right).$$

The values of G_K factors are $G_S^{(u,p)}=G_S^{(d,n)}=5.1$, $G_S^{(d,p)}=G_S^{(u,n)}=4.3$, $G_S^{(s,p)}=G_S^{(s,n)}=2.5$, $G_V^{(u,p)}=G_V^{(d,n)}=2$, $G_V^{(d,p)}=G_V^{(u,n)}=1$. The $g_{XK(q)}$ coefficients can be written as combinations of Wilson coefficients

$$g_{LV(q)} = \frac{\sqrt{2}}{G_F} \left(e^2 Q_q (K_1^L - K_2^R) - \frac{1}{2} (C_{llqq}^{VLL} + C_{llqq}^{VLR}) \right), g_{LS(q)} = -\frac{\sqrt{2}}{2G_F} \left(C_{llqq}^{SLL} + C_{llqq}^{SLR} \right),$$

where Q_q are the electric charge of quarks, C_{llqq}^{SLL} equals B_{XY}^K (C_{XY}^K) for d-quarks (u-quarks), $g_{RV(q)} = g_{LV(q)}|L \rightarrow R$ and $g_{RS(q)} = g_{LS(q)}|L \rightarrow R$.

TABLE I: Effective atomic charges, nuclear form factors and capture rates.

Nucleus	${}^A_Z\text{N}$	${}^{27}_{13}\text{Al}$	${}^{48}_{22}\text{Ti}$	${}^{80}_{38}\text{Sb}$	${}^{121}_{51}\text{Sr}$	${}^{197}_{79}\text{Au}$	${}^{208}_{82}\text{Pb}$
Z_{eff}		11.5	17.6	25	29	33.5	34
F_p		0.64	0.54	0.39	0.32	0.16	0.15
$\Gamma_{capt} \times 10^{18}$		0.464079	1.70422	4.61842	6.71711	8.59868	8.84868

III. NUMERICAL ANALYSIS

We now turn to the numerical analysis of the one loop corrections to $\mu - e$ conversion in nuclei in MRSSM by using the full evaluation within the framework of SARAH-4.14.3 [55–57] and SPheno-4.0.4 [59, 60]. The computation is done in a low scale version of SPheno and

all free parameters are given at the SUSY scale. The experimental values of Higgs mass and W boson mass can impose stringent and nontrivial constraints on the model parameters. The one loop and leading two loop corrections to the lightest (SM-like) Higgs boson in MRSSM have been computed in Ref.[38] and the new fields and couplings can give large contributions to the Higgs mass even for stop masses of order 1 TeV and no stop mixing. Meanwhile, the new fields and couplings can not give too large a contribution to the W boson mass and muon decay in the same regions of parameter space. A better agreement with the latest experimental value for W boson mass has been investigated in Ref.[41]. It combines all numerically relevant contributions that are known in SM in a consistent way with all MRSSM one loop corrections. A set of updated benchmark point BMP1 is given in Ref.[41] and we display them in Eq.(13) where all mass parameters are in GeV or GeV^2 .

$$\begin{aligned}
&\tan \beta = 3, B_\mu = 500^2, \lambda_d = 1.0, \lambda_u = -0.8, \Lambda_d = -1.2, \Lambda_u = -1.1, \\
&M_D^B = 550, M_D^W = 600, \mu_d = \mu_u = 500, v_S = 5.9, v_T = -0.33, \\
&(m_l^2)_{11} = (m_l^2)_{22} = (m_l^2)_{33} = (m_r^2)_{11} = (m_r^2)_{22} = (m_r^2)_{33} = 1000^2, \\
&(m_{\tilde{q}}^2)_{11} = (m_{\tilde{u}}^2)_{11} = (m_{\tilde{d}}^2)_{11} = (m_{\tilde{q}}^2)_{22} = (m_{\tilde{u}}^2)_{22} = (m_{\tilde{d}}^2)_{22} = 2500^2, \\
&(m_{\tilde{q}}^2)_{33} = (m_{\tilde{u}}^2)_{33} = (m_{\tilde{d}}^2)_{33} = 1000^2, m_T = 3000, m_S = 2000.
\end{aligned} \tag{13}$$

In following numerical analysis, the values in Eq.(13) will be used for all results. Note that, the off-diagonal entries of squark mass matrices $m_{\tilde{q}}^2$, $m_{\tilde{u}}^2$, $m_{\tilde{d}}^2$ and slepton mass matrices m_l^2 , m_r^2 in Eq.(13) are zero, i.e., the flavour mixing of squark and slepton is absent.

Similarly to most supersymmetry models, the LFV processes in MRSSM originate from the off-diagonal entries of the soft breaking terms m_l^2 and m_r^2 , which are parameterized by mass insertion

$$(m_l^2)_{IJ} = \delta_l^{IJ} \sqrt{(m_l^2)_{II}(m_l^2)_{JJ}}, (m_r^2)_{IJ} = \delta_r^{IJ} \sqrt{(m_r^2)_{II}(m_r^2)_{JJ}}, \tag{14}$$

where $I, J = 1, 2, 3$. To decrease the number of free parameters involved in our calculation, we assume that the off-diagonal entries of m_l^2 and m_r^2 in Eq.(14) are equal, i.e., $\delta_l^{IJ} = \delta_r^{IJ} = \delta^{IJ}$. The experimental limits on LFV decays, such as radiative two body decays $l_2 \rightarrow l_1 \gamma$, leptonic three body decays $l_2 \rightarrow 3l_1$, can give strong constraints on the parameters δ^{IJ} . In the following, we will use LFV decays $\mu \rightarrow e \gamma$ to constrain the parameters δ^{12} which has been discussed in Ref.[53]. It is noted that δ^{23} and δ^{13} have been set zero in following discussion since they have no effect on the predictions of $\text{CR}(\mu - e, \text{Nucleus})$. Current limits

of LFV decays $\mu \rightarrow e\gamma$ is $\text{BR}(\mu \rightarrow e\gamma) < 4.2 \times 10^{-13}$ from MEG [61] and new sensitivity for this decay channel in the future projects will be $\text{BR}(\mu \rightarrow e\gamma) \sim 6 \times 10^{-14}$ from MEG II [62].

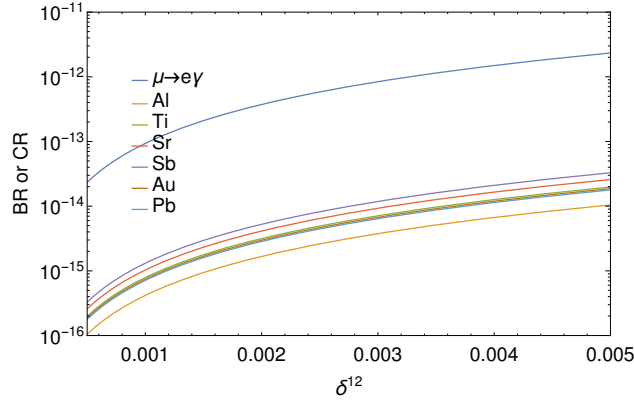


FIG. 2: Dependence of $\text{BR}(\mu \rightarrow e\gamma)$ and $\text{CR}(\mu - e, \text{Nucleus})$ on mass insertion parameter δ^{12} .

In FIG.2 the predictions for $\text{BR}(\mu \rightarrow e\gamma)$ and $\text{CR}(\mu - e, \text{Nucleus})$ for Al, Ti, Sr, Sb, Au, and Pb are shown as a function of mass insertion parameter δ^{12} . The prediction for $\text{BR}(\mu \rightarrow e\gamma)$ exceeds the future experiment sensitivity at $\delta^{12} \sim 0.001$. In a recent Ref.[53] the analytical computation and discussion of $\text{BR}(\mu \rightarrow e\gamma)$ in MRSSM has been performed. The valid region for δ^{12} in Ref.[53] calculated with the Mathematica package Package-X is compatible with that in this work calculated with SARAH and SPheno. We clearly see that both the predictions for $\text{BR}(\mu \rightarrow e\gamma)$ and $\text{CR}(\mu - e, \text{Nucleus})$ in nuclei are sensitive to δ^{12} , and they increase along with the increase of δ^{12} which have a same behavior as those in most SUSY models(e.g. [63]). At $\delta^{12} \sim 0.001$, the prediction on $\text{BR}(\mu \rightarrow e\gamma)$ is very close to the current experimental limit, and the predictions on $\text{CR}(\mu - e, \text{Nucleus})$ are around $10^{-15} - 10^{-16}$ which are two orders of magnitude below current experimental limits. The predicted $\text{CR}(\mu - e, \text{Nucleus})$ for Ti is around 10^{-15} and this is three orders of magnitude above future experimental sensitivity [4]. The predicted $\text{CR}(\mu - e, \text{Nucleus})$ for Al is around 10^{-16} and this is in region of the future experimental sensitivity [5, 6].

Taking $\delta^{12} = 0.001$, the predictions for $\text{BR}(\mu \rightarrow e\gamma)$ and $\text{CR}(\mu - e, \text{Nucleus})$ for Al, Ti, Sr, Sb, Au, and Pb are shown in FIG.3 as a function of the diagonal entries m_l of the soft breaking term m_l^2 and m_r^2 . Here, $m_l = \sqrt{(m_l^2)_{11}} = \sqrt{(m_l^2)_{22}} = \sqrt{(m_l^2)_{33}} = \sqrt{(m_r^2)_{11}} = \sqrt{(m_r^2)_{22}} = \sqrt{(m_r^2)_{33}}$. We clearly see that both the predictions for $\text{BR}(\mu \rightarrow e\gamma)$ and $\text{CR}(\mu - e, \text{Nucleus})$ in nuclei are sensitive to m_l , and they decrease along with the increase of m_l which have a same behavior as those in Ref.[63]. At $m_l = 1$ TeV, the prediction on $\text{BR}(\mu \rightarrow e\gamma)$ is below 10^{-13} . Thus, all points in plot of $\text{BR}(\mu \rightarrow e\gamma)$ are compatible with the current

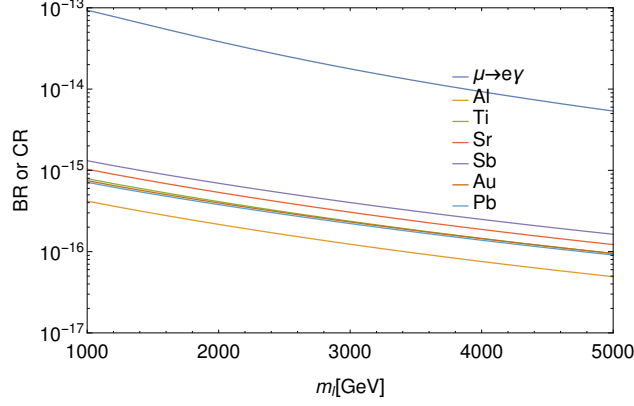


FIG. 3: Dependence of $\text{BR}(\mu \rightarrow e\gamma)$ and $\text{CR}(\mu - e, \text{Nucleus})$ on mass parameter m_l .

experimental limit. At $m_l = 5$ TeV, the predicted $\text{CR}(\mu - e, \text{Nucleus})$ for Ti is around 10^{-16} and this is still two orders of magnitude above future experimental sensitivity [4]. At $m_l = 5$ TeV, the predicted $\text{CR}(\mu - e, \text{Nucleus})$ for Al is below 10^{-16} and this is still in region of the future experimental sensitivity [5, 6].

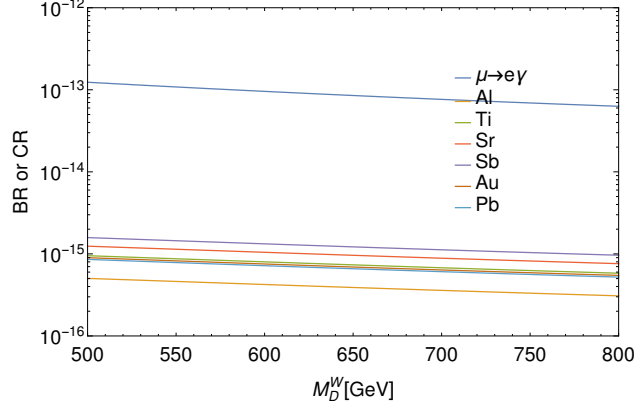


FIG. 4: Dependence of $\text{BR}(\mu \rightarrow e\gamma)$ and $\text{CR}(\mu - e, \text{Nucleus})$ on mass parameter M_D^W .

In FIG.4 the predictions for $\text{BR}(\mu \rightarrow e\gamma)$ and $\text{CR}(\mu - e, \text{Nucleus})$ are shown as a function of the wino-triplino mass parameter M_D^W . M_D^W is a new parameter introduced in MRSSM. We clearly see that both the predictions for $\text{BR}(\mu \rightarrow e\gamma)$ and $\text{CR}(\mu - e, \text{Nucleus})$ in nuclei show a weak dependence on M_D^W , and they decrease slowly along with the increase of M_D^W .

In FIG.5 the predictions for $\text{BR}(\mu \rightarrow e\gamma)$ and $\text{CR}(\mu - e, \text{Nucleus})$ are shown as a function of $\tan\beta$. We clearly see that both the predictions for $\text{BR}(\mu \rightarrow e\gamma)$ and $\text{CR}(\mu - e, \text{Nucleus})$ in nuclei are not sensitive to $\tan\beta$, and they take values along a narrow band. This is a striking difference to MSSM [42]. Due to the existence of the transition from d -Higgsino to u -Higgsino in MSSM, which is governed by μ -term, the well-known $\tan\beta$ -enhancement is

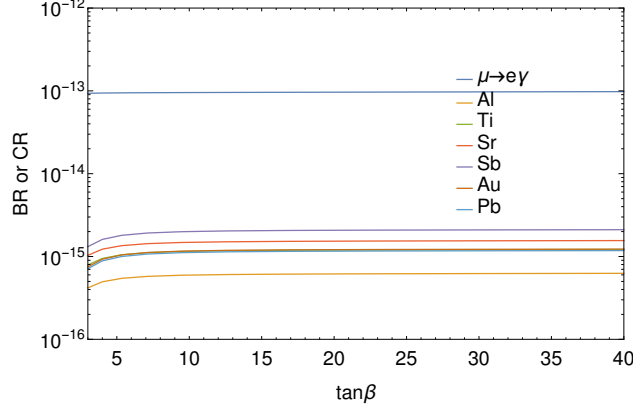


FIG. 5: Dependence of $\text{BR}(\mu \rightarrow e\gamma)$ and $\text{CR}(\mu - e, \text{Nucleus})$ on $\tan\beta$.

possible. A well-established way to understand the $\tan\beta$ -enhancement is provided by mass-insertion diagrams involving insertions of the μ -parameter and Majorana gaugino masses. However, the μ -term and Majorana gaugino masses are forbidden in MRSSM and this leads to the result that $\text{BR}(\mu \rightarrow e\gamma)$ and $\text{CR}(\mu - e, \text{Nucleus})$ are not enhanced by $\tan\beta$.

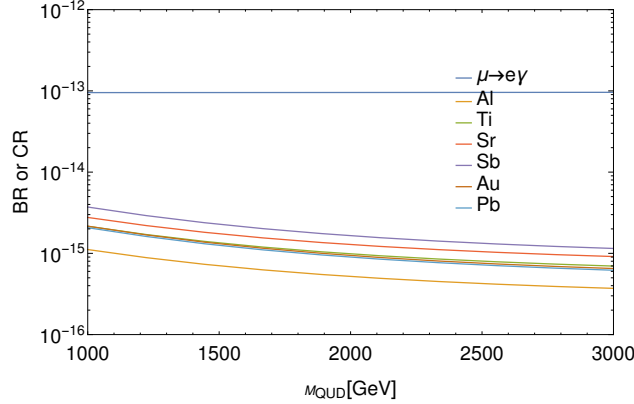


FIG. 6: Dependence of $\text{BR}(\mu \rightarrow e\gamma)$ and $\text{CR}(\mu - e, \text{Nucleus})$ on mass parameter M_{QUD} .

In FIG.6 the predictions for $\text{BR}(\mu \rightarrow e\gamma)$ and $\text{CR}(\mu - e, \text{Nucleus})$ are shown as a function of the squark mass M_{QUD} . Here, $M_{QUD} = \sqrt{(m_q^2)_{11}} = \sqrt{(m_u^2)_{11}} = \sqrt{(m_d^2)_{11}} = \sqrt{(m_q^2)_{22}} = \sqrt{(m_u^2)_{22}} = \sqrt{(m_d^2)_{22}} = \sqrt{(m_q^2)_{33}} = \sqrt{(m_u^2)_{33}} = \sqrt{(m_d^2)_{33}}$. We clearly see that the predictions for $\text{BR}(\mu \rightarrow e\gamma)$ is not sensitive to M_{QUD} , and it takes values along a narrow band. This is because there is no squark mediated diagram contributing to $\mu \rightarrow e\gamma$. Only the box diagrams contributing to $\text{CR}(\mu - e, \text{Nucleus})$ depend on the squark masses. The predictions for $\text{CR}(\mu - e, \text{Nucleus})$ show a weak dependence on M_{QUD} , and they decrease slowly along with the increase of M_{QUD} which have a baseline behaviour as those in Ref.[42].

We are also interesting to the effects from other parameters on the predictions of $\text{CR}(\mu -$

$e, \text{Nucleus})$ in MRSSM. By scanning over these parameters, such as B_μ , M_D^B , λ_d , λ_u , Λ_d , Λ_u, μ_d and μ_u , it shows the predictions for $\text{CR}(\mu - e, \text{Nucleus})$ take values along a narrow band in valid regions.

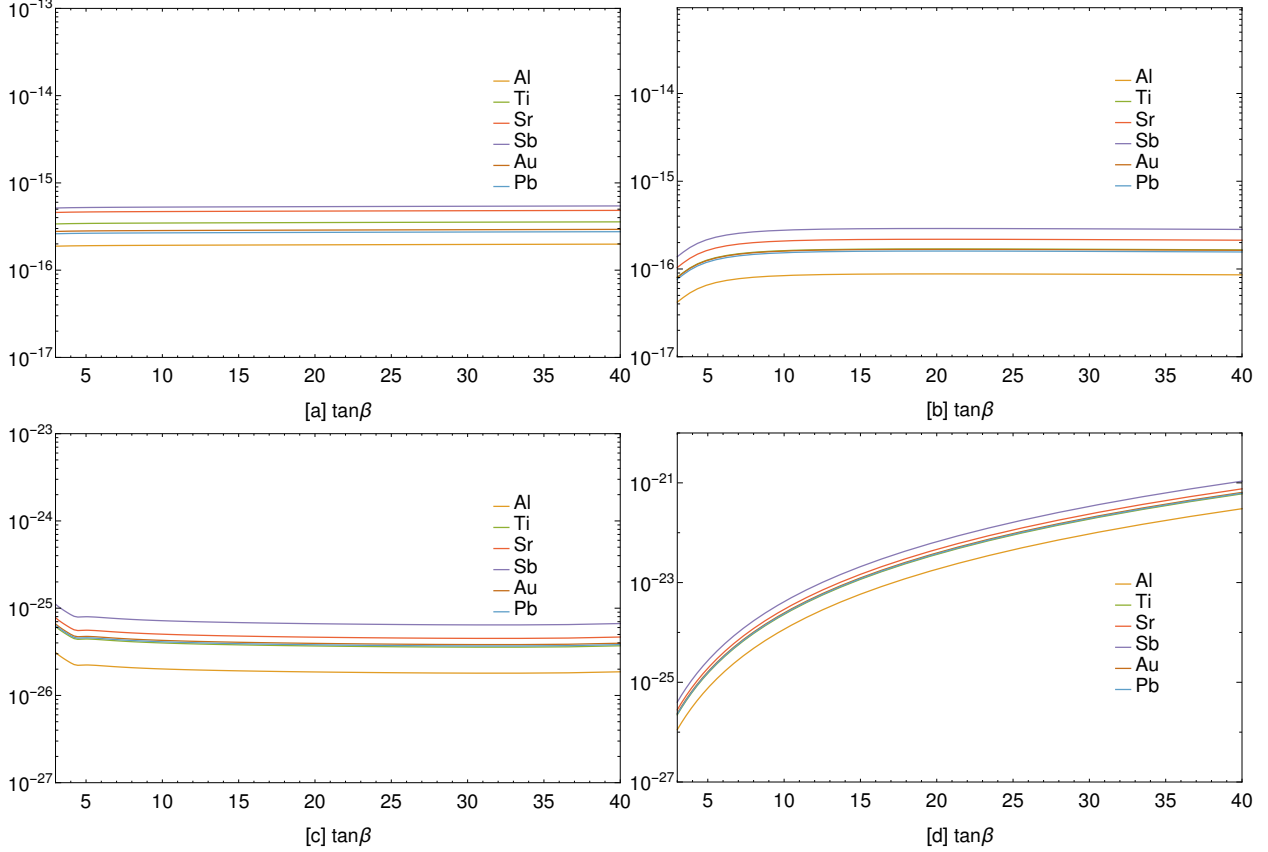


FIG. 7: Predictions on $\text{CR}(\mu - e, \text{Nucleus})$ as a function of $\tan \beta$ from various parts: [a] γ penguins; [b] Z penguins; [c] Higgs penguins; [d] box diagrams.

In FIG.7, we show the predictions on $\text{CR}(\mu - e, \text{Nucleus})$ as a function of $\tan \beta$ with the same parameter setup in FIG.5 but independently considering the contributions from each diagram, and the values of $\text{CR}(\mu - e, \text{Nucleus})$ are given by only the listed contribution with all others set to zero. The predictions on $\text{BR}(\mu \rightarrow e\gamma)$ are not displayed cause they only receive the contribution from γ penguins. We observe that the γ penguins dominate the predictions on $\text{CR}(\mu - e, \text{Nucleus})$ and the contributions from Higgs penguins and box diagrams are negligible. The Z penguins are less dominant in the predictions on $\text{CR}(\mu - e, \text{Nucleus})$ in a large parameter region. The decrease for total predictions $\text{CR}(\mu - e, \text{Nucleus})$ at $\tan \beta < 5$ in FIG.5 can be explained by a cancellation of predictions between γ penguins and Z penguins shown in FIG.7 [a] and [b].

IV. CONCLUSIONS

In this work, taking account of the constraints from $\mu \rightarrow e\gamma$ on the parameter space, we analyze the LFV process $\text{CR}(\mu - e, \text{Nucleus})$ in the framework of the Minimal R-symmetric Supersymmetric Standard Model.

In MRSSM, the theoretical predictions on $\text{CR}(\mu - e, \text{Nucleus})$ mainly depend on the mass insertion δ^{12} . The predictions on $\text{CR}(\mu - e, \text{Nucleus})$ would be zero if $\delta^{12}=0$ is assumed. Taking account of experimental bounds on radiative decays $\mu \rightarrow e\gamma$, the values of δ^{12} is constrained around 0.001. Assuming $\delta^{12} = 0.001$ and other parameter settings in Eq.(13), the predictions on $\text{CR}(\mu - e, \text{Nucleus})$ are at the level of $\mathcal{O}(10^{-15} - 10^{-16})$, which are two or three orders of magnitude above the future experimental prospects for a Al or Ti target. Thus, the LFV processes $\mu - e$ conversion in Al and Ti are very promising to be observed in near future experiment.

Acknowledgments

The work has been supported partly by the National Natural Science Foundation of China (NNSFC) under Grant Nos.11905002, 11805140 and 11705045, the Scientific Research Foundation of the Higher Education Institutions of Hebei Province under Grant No. BJ2019210, the Foundation of Baoding University under Grant No. 2018Z01, the youth top-notch talent support program of the Hebei Province.

-
- [1] S. Ahmad et al., Phys. Rev. Lett. 59(1987)970.
 - [2] W. Bertl, Eur. Phys. J. C47(2006)337.
 - [3] DM. Aoki, AIP Conf. Proc. 1441(2012)599.
 - [4] R. J. Barlow, Nucl. Phys. Proc. Suppl. 218(2011)44.
 - [5] L. Bartoszek, et al., arXiv:1501.05241.
 - [6] A. Kurup, Nucl. Phys. Proc. Suppl. 218(2011)38.
 - [7] Riazuddin, R. E. Marshak, R. N. Mohapatra, Phys. Rev. D 24 (1981) 1310.
 - [8] L. N. Chang, D. Ng, J. N. Ng, Phys. Rev. D 50 (1994) 4589.
 - [9] A. Ioannisian, A. Pilaftsis, Phys. Rev. D 62 (2000) 066001.

- [10] A. Pilaftsis, T. E. J. Underwood, Phys. Rev. D 72 (2005) 113001.
- [11] F. Deppisch, T. S. Kosmas, J. W. F. Valle, Nucl. Phys. B 752 (2006) 80.
- [12] A. Ilakovac, A. Pilaftsis, Phys. Rev. D 80 (2009) 091902.
- [13] F. F. Deppisch, A. Pilaftsis, Phys. Rev. D 83 (2011) 076007.
- [14] M. Raidal, A. Santamaria, Phys. Lett. B 421 (1998) 250.
- [15] E. Ma, M. Raidal, U. Sarkar, Nucl. Phys. B 615 (2001) 313.
- [16] D. N. Dinh, A. Ibarra, E. Molinaro, S. T. Petcov, JHEP08(2012)125, JHEP 09 (2013) 023 (erratum).
- [17] K.-S. Sun, T.-F. Feng, G.-H. Luo, X.-Y. Yang, J.-B. Chen, Mod.Phys.Lett. A28 (2013) 1350151.
- [18] A. Abada, C. Biggio, F. Bonnet, M. B. Gavela, T. Hambye, Phys. Rev. D 78 (2008)033007.
- [19] G.-J. Ding, M.-L. Yan, Phys.Rev. D77 (2008) 014005.
- [20] K.-S. Sun, T.-F. Feng, L.-N. Kou, F. Sun, T.-J. Gao, H.-B. Zhang, Mod.Phys.Lett. A 27 (2012) 1250172.
- [21] M. Blanke, A. J. Buras, B. Duling, A. Poschenrieder, C. Tarantino, JHEP 0705(2007)013.
- [22] F. D. Aguila, J. I. Illana, M. D. Jenkins, JHEP 1103(2011)080.
- [23] C. Bonilla, M. E. Krauss, T. Opferkuch, W. Porod, JHEP 1703 (2017) 027.
- [24] D. T. Huong, D. N. Dinh, L. D. Thien, P. V. Dong, JHEP 08(2019)051.
- [25] J. Hisano, S. Sugiyama, M. Yamanaka, M. J. S. Yang, Phys. Lett. B 694(2011)380.
- [26] J. Sato, M. Yamanaka, Phys.Rev. D91(2015)055018.
- [27] A. Ilakovac, A. Pilaftsis, L. Popov, Phys. Rev. D87 (2013) 053014.
- [28] T. Guo, S.-M. Zhao, X.-X. Dong, C.-G. Duan, T.-F. Feng, Eur.Phys.J.C 78 (2018)925.
- [29] X.-X. Dong, S.-M. Zhao, H.-B. Zhang, T.-F. Feng, Eur.Phys.J.C 79 (2019)17.
- [30] E. Arganda, M.J. Herrero, A.M. Teixeira, JHEP0710(2008)104.
- [31] H.-B. Zhang, T.-F. Feng, G.-H. Luo, Z.-F. Ge, and S.-M. Zhao, JHEP 1307 (2013)069.
- [32] L. Calibbi, G. Signorelli, Riv.Nuovo Cim. 41(2018)1.
- [33] R. H. Bernstein, P. S. Cooper, Phys.Rept. 532 (2013) 27.
- [34] M. Lindner, M. Platscher, F. S. Queiroz, Phys.Rept. 731 (2018)1.
- [35] G. D. Kribs, E. Poppitz, N. Weiner, Phys. Rev. D 78 (2008) 055010.
- [36] P. Diessner, W. Kotlarski, PoS CORFU2014 (2015) 079.
- [37] P. Diessner, J. Kalinowski, W. Kotlarski, D. Stöckinger, Adv.High Energy Phys. 2015 (2015)

760729.

- [38] P. Diessner, J. Kalinowski, W. Kotlarski, D. Stöckinger, JHEP1412(2014)124.
- [39] P. Diessner, W. Kotlarski, S. Liebschner, D. Stöckinger, JHEP1710(2017)142.
- [40] P. Diessner, J. Kalinowski, W. Kotlarski, D. Stöckinger, JHEP1603(2016)007.
- [41] P. Diessner, G. Weiglein, JHEP 1907 (2019) 011.
- [42] W. Kotlarski, D. Stöckinger, H. Stöckinger-Kim, JHEP 1908 (2019) 082.
- [43] A. Kumar, D. Tucker-Smith, N. Weiner, JHEP 1009 (2010) 111.
- [44] A. E. Blechman, Mod.Phys.Lett. A24 (2009)633.
- [45] G. D. Kribs, A. Martin, T. S. Roy, JHEP 0906 (2009) 042.
- [46] C. Frugiuele, T. Gregoire, Phys.Rev. D85 (2012) 015016.
- [47] J. Kalinowski, Acta Phys.Polon. B47 (2016) 203.
- [48] S. Chakraborty, A. Chakraborty, S. Raychaudhuri, Phys.Rev. D94 (2016) 035014.
- [49] J. Braathen, M. D. Goodsell, P. Slavich, JHEP 1609 (2016) 045.
- [50] P. Athron, J.-hyeon Park, T. Steudtner, D. Stöckinger, A. Voigt, JHEP 1701 (2017) 079.
- [51] C. Alvarado, A. Delgado, A. Martin, Phys.Rev. D97 (2018)115044.
- [52] K.-S. Sun, J.-B. Chen, X.-Y. Yang, H.-B. Zhang, Mod. Phys. Lett. A 34(2019)1950058.
- [53] K.-S. Sun, J.-B. Chen, X.-Y. Yang, S.-K. Cui, Chin. Phys. C 43(2019)043101.
- [54] K.-S. Sun, J.-B. Chen, H.-B. Zhang, Sheng-Kai Cui, Mod. Phys. Lett. A 35(2020)1950358.
- [55] F. Staub, arXiv:0806.0538.
- [56] F. Staub, Comput. Phys. Commun. 184 (2013) 1792.
- [57] F. Staub, Comput. Phys. Commun. 185 (2014) 1773.
- [58] W. Porod, F. Staub, A. Vicente, Eur.Phys.J. C74(2014)2992.
- [59] W. Porod, Comput. Phys. Commun. 153 (2003) 275.
- [60] W. Porod, F. Staub, Comput. Phys. Commun. 183 (2012) 2458.
- [61] A. M. Baldini, et al., (MEG Collaboration), Eur. Phys. J. C76 (2016)434.
- [62] A. M. Baldini, et al, (MEG Collaboration), Eur. Phys. J. C78(2018)380.
- [63] K.-S. Sun, T.-F. Feng, T.-J. Gao, S.-M. Zhao, Nucl. Phys. B 865 (2006)486.